



Geophysical Research Letters

RESEARCH LETTER

10.1002/2017GL075003

Key Points:

- Hybrid flashes have statistically different size and altitude distributions from intracloud and cloud-to-ground flashes
- Hybrid flashes initially have electric field properties similar to intracloud flashes but produce a return stroke
- Due to their larger sizes, hybrid flashes produce ≥159% more nitrogen oxides than intracloud and cloud-to-ground flashes

Correspondence to:

R. M. Mecikalski, retha.mecikalski@nsstc.uah.edu

Citation

Mecikalski, R. M., Bitzer, P. M., & Carey, L. D. (2017). Why flash type matters: A statistical analysis. *Geophysical Research Letters*, 44. https://doi.org/10.1002/ 2017GL075003

Received 18 JUL 2017 Accepted 4 SEP 2017 Accepted article online 7 SEP 2017

Why Flash Type Matters: A Statistical Analysis

Retha M. Mecikalski¹, Phillip M. Bitzer¹, and Lawrence D. Carey¹

¹Atmospheric Science Department, University of Alabama in Huntsville, Huntsville, AL, USA

Abstract While the majority of research only differentiates between intracloud (IC) and cloud-to-ground (CG) flashes, there exists a third flash type, known as hybrid flashes. These flashes have extensive IC components as well as return strokes to ground but are misclassified as CG flashes in current flash type analyses due to the presence of a return stroke. In an effort to show that IC, CG, and hybrid flashes should be separately classified, the two-sample Kolmogorov-Smirnov (KS) test was applied to the flash sizes, flash initiation, and flash propagation altitudes for each of the three flash types. The KS test statistically showed that IC, CG, and hybrid flashes do not have the same parent distributions and thus should be separately classified. Separate classification of hybrid flashes will lead to improved lightning-related research, because unambiguously classified hybrid flashes occur on the same order of magnitude as CG flashes for multicellular storms.

1. Introduction

Traditionally, lightning is classified into two major types: intracloud (IC) and cloud-to-ground (CG). This classification has been used in a variety of applications, such as their relationship to kinematic and microphysical properties of convective storms, severe weather forecasting, climatological research, and more. Further, lightning modeling studies and their related lightning-produced nitrogen oxides (LNOx) have relied on this classification. Past LNOx modeling studies suggest that there is either roughly an order of magnitude difference in LNOx production between IC and CG flashes or IC and CG flashes produce the same amount of LNOx. Specifically, Pickering et al. (1998) showed that IC and CG flashes produced 113 and 1,113 moles flash⁻¹, respectively; Koshak et al. (2014) obtained values of 34.78 and 484.15 moles flash⁻¹, respectively; and Carey et al. (2016) obtained values of 116 and 919 moles flash⁻¹, respectively. Conversely, Barthe and Barth (2008), DeCaria et al. (2005), and Ott et al. (2007) showed that IC and CG flashes produced the same amount of LNOx. However, these and other studies only compared IC to CG flashes, but a third type of flash, called hybrid flashes, exists, e.g., Bitzer et al. (2013), Boggs et al. (2016), Maggio et al. (2005), Lang et al. (2013), Lu et al. (2012), and Mecikalski and Carey (2017). Maggio et al. (2005) compared Lightning Mapping Array (LMA) data to electric field change sensors for various flashes, including hybrid flashes, while Lu et al. (2012) found that negative strokes with the largest impulse charge moment changes were mostly produced by hybrid flashes that had an initial, extensive IC component located at higher altitudes than observed for CG flashes; these hybrid flashes would thus be more likely to produce sprites than CG flashes (Boggs et al., 2016; Lang et al., 2013). Therefore, although the lightning community is aware of hybrid flashes, the LNOx community has not yet included hybrid flashes in their studies (e.g., Barthe & Barth, 2008; Barth et al., 2007; Cummings et al., 2013; Ott et al., 2007). Nevertheless, while Carey et al. (2016) only compared IC and CG flashes in their LNOx analysis, they mentioned that hybrid flashes occurred during periods of larger CG LNOx production. These hybrid flashes are a combination of an IC and a CG flash; they usually travel large horizontal distances within a cloud (the IC component) and have a return stroke to ground (the CG component). Thus, hybrid flashes are grouped in the CG category in current LNOx methodologies due to their return strokes to ground. If the above LNOx parameterization studies (e.g., Carey et al., 2016; DeCaria et al., 2005; Koshak et al., 2014; Ott et al., 2007; Pickering et al., 1998) were reanalyzed using hybrid flashes as the third flash type, instead of grouping hybrid flashes with CGs, significantly different LNOx per flash type could be obtained.

There is a renewed interest in how lightning characteristics influence NO_x and other chemical species, including recent studies emanating from the Deep Convective Cloud and Chemistry (DC3) experiment (e.g., Barth et al., 2015; Carey et al., 2016; DiGangi et al., 2016; Mecikalski et al., 2015; Mecikalski & Carey, 2017; Pollack et al., 2016; Stith et al., 2016). However, as mentioned, only Mecikalski and Carey (2017) separately classified hybrid flashes from CG flashes in their study. They showed through use of histogram analyses that (1) IC, CG,

©2017. American Geophysical Union. All Rights Reserved.



and hybrid flashes have different peaks in their distributions, both as a function of altitude and reflectivity; (2) hybrid flashes occur more often than CG flashes in stronger convective storms such as mesoscale convective systems (MCSs) and supercells; and (3) hybrid flashes have larger spatial extents than IC and CG flashes. Specifically, Mecikalski and Carey (2017) showed that when hybrid flashes are separately classified from CG flashes, the peak of the distribution for CG flash initiation altitudes is roughly 5° C in multicells and -5° C in MCSs and supercells compared to the -15° C used in, e.g., DeCaria et al. (2000, 2005) and Ott et al. (2010), when hybrid flashes were not separately classified. Further, CG flashes propagate within regions of higher radar reflectivities as compared to hybrid flashes (Mecikalski & Carey, 2017). Therefore, if hybrid flashes are grouped with CG flashes, then the altitudes where CG flashes initiate and propagate will be erroneously biased to higher altitudes, while also leading to errors in model output related to flash size and radar reflectivity values. The research herein is therefore focused on statistically showing that IC, CG, and hybrid flashes do not have the same parent distribution relative to their respective flash sizes, and where these flashes initiate and propagate, suggesting that hybrid flashes need to be separately classified from CG flashes, which has not been done in prior LNOx studies.

2. Data and Methodology

Hybrid flashes can be classified by using a combination of data from electric field waveforms in the very low frequency to low frequency (VLF/LF) range (such as the Huntsville Alabama Marx Meter Array (HAMMA) and the National Lightning Detection Network (NLDN)) and by using data from the very high frequency (VHF) range, such as LMA or lightning detection and ranging instruments. As such, three data sets were used in this study: (1) The North Alabama LMA (NALMA) (Goodman et al., 2005; Koshak et al., 2004), (2) NLDN (Cummins & Murphy, 2009; Cummins et al., 1998, 2006), and (3) HAMMA (Bitzer et al., 2013). NALMA detects radiation from leader breakdown processes in the VHF range. The flash detection efficiency (DE) is >90% (Chmielewski & Bruning, 2016) and horizontal and vertical location accuracy (LA) is ≤0.5 km and on the order of 1 km, respectively, within 100 km of the center of NALMA (Koshak et al., 2004). Thus, only flashes that initiated within 100 km of the center of NALMA were used. NLDN operates in the VLF/LF range and detects radiation from discharges whose magnetic field amplitudes exceed certain sensor thresholds, such as return strokes (and K changes). NLDN has flash DE of \sim 95% and LA <0.5 km across the continental United States (Cummins et al., 2006; Cummins & Murphy, 2009; Mallick et al., 2014). HAMMA is an array of broadband electric field change meters that also operates in the VLF/LF range; it records the radiation, induction, and electrostatic components of the electric field from nearby lightning (Bitzer et al., 2013). HAMMA archives the electric field waveforms, making it a beneficial data set to compare to other flash classification algorithms in postprocessing.

HAMMA can be used to classify flashes due to variations in the electric field waveforms for IC, CG, and hybrid flashes. For instance, IC flashes have mostly unipolar pulses during the preliminary breakdown (PB) process, while the initial half cycles of the pulses are usually positive (for normal IC flashes) with much larger amplitudes compared to the second half cycles. IC flashes also do not have a return stroke to ground (an example of what this looks like in HAMMA is shown in Figure 1a herein). CG flashes have bipolar pulses during the PB process, with negative initial half cycles (for a —CG flash), while the amplitudes of the pulses in the second half cycles are comparable to the amplitudes of the initial half cycles and eventually have at least one return stroke (Figure 1b). Hybrid flashes are a combination of IC and CG flashes; initially multiple unipolar pulses (with positive initial half cycles) similar to ICs are detected, while eventually, there would also be at least one return stroke to ground (Figure 1c).

In this study, xlma (Thomas et al., 2003) was used for flash sorting and classification, and the convex hull area (Bruning & MacGorman, 2013; Mecikalski et al., 2015; Mecikalski & Carey, 2017) was used for flash area and extent calculations. NALMA VHF sources were clustered into flashes using \geq 10 VHF sources with spatial and temporal constraints of no more than 3 km in the x, y, and z directions and 0.15 s between VHF sources, with a maximum of 3 s for an entire flash. For the xlma flash type classification, only NLDN CG return strokes were used and all CG return strokes between 0 and +15 kA were removed (Biagi et al., 2007; Cummins et al., 1998, 2006). Xlma classifies flashes by incorporating leader direction and speed, breakdown location (single versus bilevel), the location where 75% of the sources occurred and NLDN return stroke information (Thomas et al., 2003). For instance, xlma would classify a flash as a normal IC if it initiated at higher

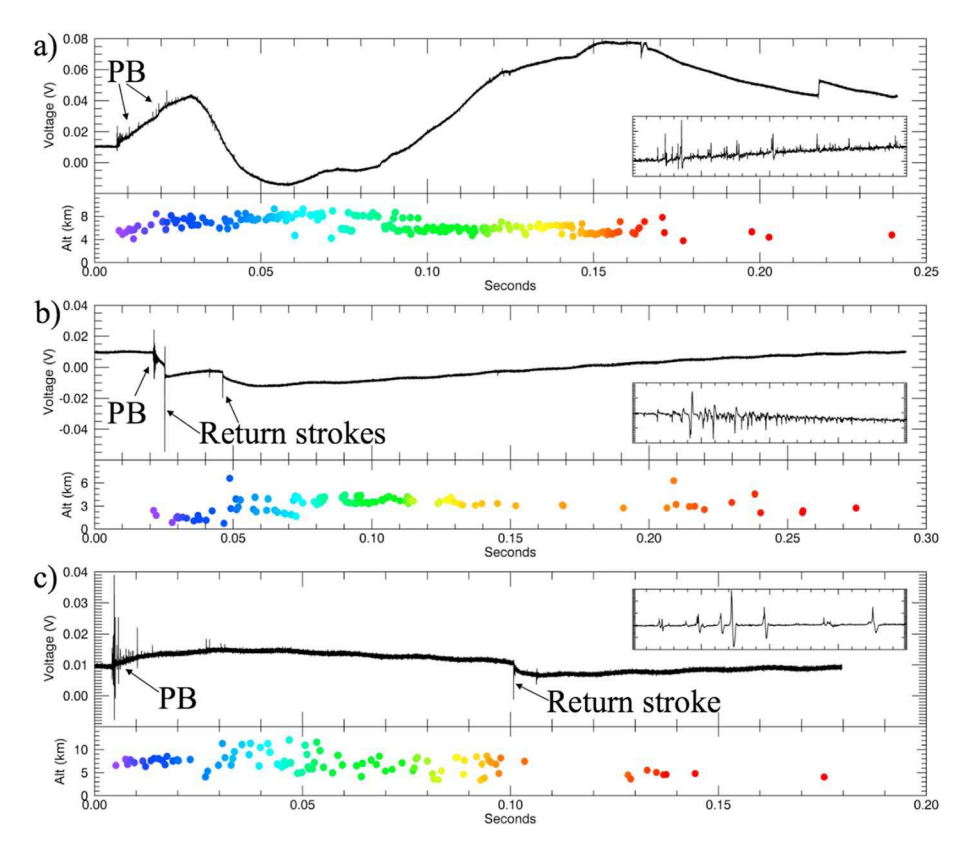


Figure 1. Examples of HAMMA electric field waveforms (black lines) and xlma NALMA VHF sources (color-coded circles according to time) for an (a) IC, (b) CG, and (c) hybrid flash. For each flash, the inset figure shows the first 2 ms of the flash, highlighting the PB period.

altitudes (usually >6 km), the initial leader moved in the positive (upward) direction, there was bilevel breakdown in the VHF (NALMA) data, i.e., leader breakdown occurred in the lower positive and main negative charge regions of a cloud, and there was no NLDN return stroke to ground (Figure 1a). In contrast, a flash would be classified as a —CG if it initiated at lower altitudes (usually <6 km), the initial leader moves in the negative (downward) direction, there was single-level breakdown, i.e., leader breakdown occurred only in the lower positive charge region, and a negative NLDN return stroke to ground occurred (Figure 1b) (Thomas et al., 2003). Hybrid flashes are classified as such when the flash initiated at higher altitudes, the initial leader moved in the positive (upward) direction, there was bilevel breakdown in the VHF data, and there was an NLDN return stroke to ground, all of which occur within the spatial and temporal limits stated earlier (Figure 1c). Only flashes that were unambiguously classified as IC flashes (including both normal and inverted polarity), CG flashes (including both —CG and +CG) and hybrid flashes (of both negative and positive polarity) were used in the results herein in an effort to avoid including biases from "unclassified" IC or CG flashes.

In order to verify whether the output from the classified xlma flashes were the same as those observed by HAMMA, a total of 440 unambiguously xlma classified flashes (thus, IC, CG, and hybrid) were compared to the HAMMA electric field waveforms for multicell flashes that occurred on 21 May 2012. Each flash was visually inspected by colocating the xlma classified VHF NALMA sources and HAMMA electric field waveforms (as described above), and "zooming" in and out of certain parts of each flash (as in Figure 1). Repeating this process for the 440 flashes, it was determined that HAMMA confirmed the xlma classification for 96.5% (274/284) of the IC flashes, 97.1% (100/103) of the CG flashes and 98.0% (50/51) of the hybrid flashes. Ten of the flashes classified as IC's by xlma were hybrid flashes with definitive return strokes in HAMMA, while two of the xlma classified CG flashes were IC flashes and one was a hybrid flash according to HAMMA. There was also one flash that was classified as a hybrid flash by xlma, but HAMMA did not record a return stroke; this flash was an IC flash.



Based on the above results, the automated xlma classification has considerable skill when using LMA and NLDN data. As such, the scheme was applied to all unambiguously classified flashes that occurred within 100 km of the NALMA center during the month of May 2012, but taking care to only include flashes that occurred within multicellular convection. Mecikalski and Carey (2017) showed that flash characteristics vary as a function of flash type as well as storm type, and therefore, we wanted to ensure that the results presented herein were not biased due to variations in storm type. By expanding the data set, a total of 20,363 IC, 2,397 CG, and 2,200 hybrid flashes were compared to each other relative to their (1) flash sizes, (2) flash initiation altitude, and (3) all VHF source altitudes per flash type (i.e., where the flash propagates) using the two-sample Kolmogorov-Smirnov (KS) test as described in Press et al. (1992) and Wilks (2006). Thus, from this comparison of unambiguously classified flashes from May 2012, hybrid flashes occur on the same order of magnitude as CG flashes for multicellular storms.

The two-sample KS test is a nonparametric test (i.e., there is no dependency on a particular parameter, such as the mean, variance, and standard deviation, and therefore no assumptions need to be made regarding the probability distribution function type) and measures the maximum distance between the cumulative distribution function (CDF) of the two samples (Press et al., 1992; Wilks, 2006). For the two-sample KS test, the CDFs of the two samples are compared to each other; the null hypothesis is that the two samples are drawn from the same "parent" distribution (i.e., the samples have the same distribution). Hence, if the two samples have the same parent distribution, then the null hypothesis is not rejected, but if the two samples have different distributions, then the null hypothesis is rejected. The critical distance (D) is the maximum absolute difference between the empirical CDFs from the two samples; D will vary between 0 (if the samples are identical) and 1 (if there is no overlap between the samples). There are various advantages to using the two-sample KS test including as follows: (1) no assumption of the underlying distribution is required; (2) unequal sample sizes can be used because the empirical CDFs are step functions; (3) it is sensitive to differences in the location and the shape of the empirical CDFs and is thus one of the most useful and general nonparametric methods for comparing two samples, making it appropriate to use (Grenier et al., 2013; Maia et al., 2007; Press et al., 1992; Wilks, 2006).

3. Results and Discussion

The two-sample KS test was applied to IC, CG, and hybrid flashes relative to their size (Figures 2a and 2b), flash initiation altitude (Figure 2c), and flash propagation altitudes (Figure 2d); Table 1 shows the D values and the probability that these flashes come from the same parent distribution. For IC, CG, and hybrid flash comparisons, the null hypothesis for all three tests (i.e., flash size, flash initiation altitude, and flash propagation altitude) is rejected at the 99% confidence level. Therefore, IC, CG, and hybrid flashes do not have the same parent distribution, and consequently, these flashes are statistically, significantly different. In fact, Figure 2 and Table 2 show that while IC and CG flashes have similar flash areas and extents (the extent is the square root of the area), hybrid flashes have flash areas almost 3 times larger than IC and CG flashes, and flash extents almost double that of IC and CG flashes.

As an example of how LNOx calculations can be influenced when hybrid flashes are not separately classified, Table 2 also shows the total amount of NO (in moles) that each flash type would produce when using lower end values from prior research (DeCaria et al., 2005 and Skamarock et al., 2003, as listed in Schumann & Huntrieser, 2007). If only flash count is considered (at 460 moles per flash, as in DeCaria et al., 2005), then CG and hybrid flashes will produce approximately the same amount of NO; thus, one would double the amount of NO that is produced by CG flashes if hybrid flashes are not separately classified. If, on the other hand, one considers flash size (at 1.7 moles km⁻¹ of flash, as in Skamarock et al., 2003, which is a conservative number compared to others listed in Schumann & Huntrieser, 2007), then it is clear from the flashes analyzed herein that hybrid flashes produce 1.59 times more total NO than CG flashes. Therefore, if hybrid flashes are not separately classified, one would artificially increase the total amount of NO produced by CG flashes by 159%, where $P(LNOx) = Total flash size (km) \times 1.7 mol NO km⁻¹. Moreover, if one compares the median and mean amount$ of NO that would be produced per flash if one considers the median/mean flash size per flash type, then hybrid flashes would produce ≥159% and ≥170% more NO than IC and CG flashes, respectively, on a per flash basis.

DeCaria et al. (2000) noted that one of the largest sources of uncertainty in the modeling of LNOx is due to the sensitivity of LNOx mixing ratios (which is inversely proportional to the horizontal area of a flash), while Ridley

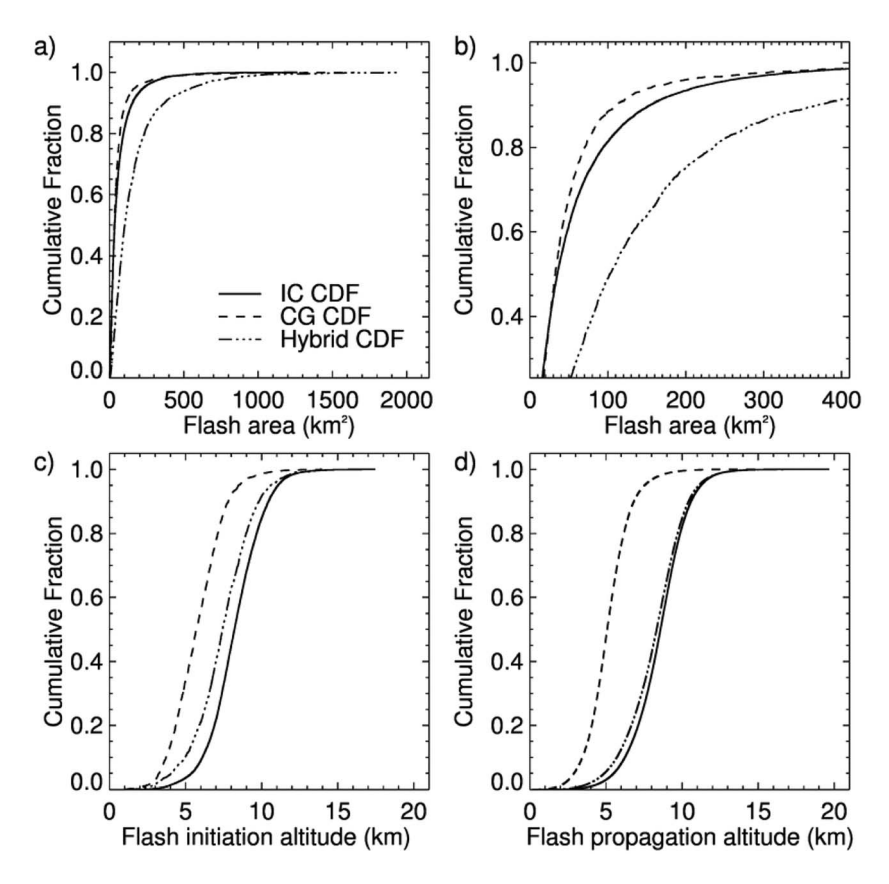


Figure 2. CDF's of IC (solid line), CG (dashed line), and hybrid (dot-dashed line) flashes comparing the (a) flash area that comprise a particular flash type for the entire distribution for all points while (b) is limited to a subset of the flash areas (emphasizing the differences between the flash types), (c) flash initiation altitudes and (d) flash propagation altitudes.

et al. (1996) stated that knowing the vertical distribution of LNOx is just as important as knowing the amount of LNOx that is produced, due to the lifetime of NO_x increasing as a function of increasing altitude. Therefore, the results herein could have significant impacts on how lightning is analyzed in observational studies and how it is applied in chemistry and modeling studies. As stated by Mecikalski and Carey (2017) if hybrid flashes are grouped with CG flashes (purely due to the presence of an NLDN return stroke), then the altitudes where CG flashes initiate and propagate will be biased to higher altitudes, while their flash sizes will be biased to larger sizes. Also, it is important to note that although this study was based on multicellular storms over northern Alabama, these hybrid flashes are not limited to only Alabama; hybrid flashes have been noted in other regions, e.g., in Florida, USA (Boggs et al., 2016), New Mexico, USA (Maggio et al., 2005), China (Qie et al., 2013), and Beijing (Zhang et al., 2015). In fact, out of 185 +CG flashes (they specifically focused on positive polarity return strokes), Qie et al. (2013) found that 36.22% were hybrid flashes. Furthermore, Mecikalski and Carey (2017) showed that these hybrid flashes are not only limited to multicellular storms but also occur in MCSs and supercells. Moreover, it was found that hybrid flashes actually occurred more often than CG flashes in MCSs and in supercells (Mecikalski & Carey, 2017), while in MCSs,

Table 1 *Results From the KS Test*

| | IC versus CG | | CG versus hybrid | | IC versus hybrid | |
|-------------|--------------|-------------|------------------|-------------|------------------|-------------|
| Property | D | Probability | D | Probability | D | Probability |
| Size | 0.0814 | 0.00% | 0.4575 | 0.00% | 0.3828 | 0.00% |
| Initiation | 0.5623 | 0.00% | 0.3865 | 0.00% | 0.1940 | 0.00% |
| Propagation | 0.7384 | 0.00% | 0.6806 | 0.00% | 0.0669 | 0.05% |

Note. Relative to flash size (km), flash initiation altitude (km), and flash propagation altitude (km), for IC, CG and hybrid flashes.

CAGU Geophysical Research Letters

Table 2 Comparison of Different IC, CG, and Hybrid Flash Properties

| Property | IC flashes | CG flashes | Hybrid flashes | CG + Hybrid flashes |
|--|------------|------------|----------------|---------------------|
| Total number of flashes | 20,363 | 2,397 | 2,200 | 4,597 |
| Total flash size (km) | 140,522 | 15,727 | 24,997 | 40,723 |
| Median area (km²) | 35.03 | 32.37 | 102.33 | 54.64 |
| Mean area (km ²) | 65.86 | 57.55 | 166.00 | 109.46 |
| Median extent (km) | 5.92 | 5.69 | 10.12 | 7.39 |
| Mean extent (km) | 8.12 | 7.59 | 12.88 | 8.86 |
| Total NO based on flash count at 460 moles per flash (moles) | 9,366,980 | 1,102,620 | 1,012,000 | 2,114,620 |
| Total NO based on total flash size at 1.7 moles km^{-1} (moles) | 238,887 | 26,735 | 42,495 | 69,231 |
| Median NO per flash based on median flash extent (moles) | 10.06 | 9.67 | 17.20 | 12.56 |
| Mean NO per flash based on mean flash extent (moles) | 13.80 | 12.90 | 21.90 | 15.06 |

Note. Mean and median flash area and flash extent for IC, CG, and hybrid flashes. Also shown is the amount of NO (moles) that each flash type would produce when using 460 moles per flash (DeCaria et al., 2005) and 1.7 moles km⁻¹ of flash, when flash size is taken into account (Skamarock et al., 2003).

hybrid flashes also had average flash extents almost double that of CG flashes. These studies show that hybrid flashes occur in a variety of environments globally and that depending on the storm type (i.e., multicellular, MCS, supercellular), their frequency of occurrence could be much higher than shown herein. Therefore, it is imperative to separately classify hybrid flashes from CG flashes.

4. Conclusions

The KS test was applied to IC, CG, and hybrid flashes relative to their size, flash initiation altitude, and flash propagation altitudes; the null hypothesis is that the two samples have the same parent distribution. It was shown that these flash types do not have the same parent distribution because the null hypothesis was rejected at the 99% confidence level for all cases. Therefore, if improved lightning and lightning-related chemistry modeling is required, or if any kind of flash type analysis is done, it is imperative that IC, CG, and hybrid flashes be separately classified and analyzed. Specifically, if hybrid flashes are grouped with CG flashes (as is currently done in most flash classification analyses), then the analyses could lead to misleading results (Table 2).

In order for more accurate flash typing and LNOx analyses to occur, it may be necessary to have data from NALMA, NLDN, and HAMMA (or similar instruments) so that more data can be tested and compared between the various lightning networks. The purpose of this would be to develop an improved methodology to classify flashes by doing multiple comparisons between what is observed by NALMA, NLDN, and HAMMA networks. While it was shown herein that xlma performed well for flashes that could be compared to HAMMA, there were several thousands of xlma classified flashes that could not be included in this study due to these flashes being ambiguously classified (i.e., they were classified as "unclassified IC," "unclassified CG," or "unclassified flash"—these flashes could be either IC, CG, or hybrid flashes). Thus, in order to reduce the number of ambiguously classified flashes, it is important to improve the classification methodologies, which would only be feasible once more comparisons, such as those presented herein, are performed.

Acknowledgments

We wish to recognize funding from the National Science Foundation's Physical and Dynamical Meteorology (NSF PDM) Program (grant AGS-1063573), which partially supported this research and supported the DC3 field experiment. Data used herein were obtained from the DC3 webpage and can be obtained here: http://data.eol.ucar.edu/master_ list/?project=DC3. Finally, we wish to thank the anonymous reviewers for their comments/suggestions that have significantly improved the paper.

References

Barth, M. C., Kim, S.-W., Wang, C., Pickering, K. E., Ott, L. E., Stenchikov, G., ... Telenta, B. (2007). Cloud-scale model intercomparison of chemical constituent transport in deep convection. Atmospheric Chemistry and Physics, 7, 4,709-4,731. https://doi.org/10.5194/acp-7-4709-2007 Barth, M. C., Cantrell, C. A., Brune, W. H., Rutledge, S. A., Crawford, J. H., Huntrieser, H., ... Ziegler, C. (2015). The deep convective clouds and chemistry (DC3) field campaign, Bulletin of the American Meteorological Society, 96, 1,281–1,309. https://doi.org/10.1175/ BAMS-D-13-00290.1

Barthe, C., & Barth, M. C. (2008). Evaluation of a new lightning-produced NO_x parameterization for cloud resolving models and its associated uncertainties. Atmospheric Chemistry and Physics, 8, 4,691-4,710. https://doi.org/10.5194/acp-8-4691-2008

Biagi, C. J., Cummins, K. L., Kehoe, K. E., & Krider, P. (2007). National lightning detection network (NLDN) performance in southern Arizona, Texas, and Oklahoma in 2003-2004. Journal of Geophysical Research, 112, D05208. https://doi.org/10.1029/2006JD007341

Bitzer, P. M., Christian, H. J., Stewart, M., Burchfield, J., Podgorny, S., Corredor, D., ... Franklin, V. (2013). Characterization and applications of VLF/LF source locations from lightning using the Huntsville Alabama Marx Meter Array. Journal of Geophysical Research: Atmospheres, 118, 3,120-3,138. https://doi.org/10.1002/jgrd.50271

Boggs, L. D., Liu, N., Splitt, M., Lazarus, S., Glenn, C., Rassoul, H., & Cummer, S. A. (2016). An analysis of five negative sprite-parent discharges and their associated thunderstorm charge structures. Journal of Geophysical Research: Atmospheres, 121, 759-784. https://doi.org/ 10.1002/2015JD024188



- Bruning, E. C., & MacGorman, D. R. (2013). Theory and observations of controls on lightning flash size spectra. *Journal of the Atmospheric Sciences*, 70, 4,012–4,029. https://doi.org/10.1175/JAS-D-12-0289.1
- Carey, L. D., Koshak, W., Peterson, H., & Mecikalski, R. M. (2016). The kinematic and microphysical control of lightning rate, extent and NO_x production. *Journal of Geophysical Research: Atmospheres, 121, 7,975–7,989.* https://doi.org/10.1002/2015JD024703
- Chmielewski, V. C., & Bruning, E. C. (2016). Lightning mapping array flash detection performance with variable receiver thresholds. *Journal of Geophysical Research: Atmospheres, 121*, 8,600–8,614. https://doi.org/10.1002/2016JD025159
- Cummings, K. A., Huntemann, T. L., Pickering, K. E., Barth, M. C., Skamarock, W. C., Höller, H., ... Schlager, H. (2013). Cloud-resolving chemistry simulation of a Hector thunderstorm. *Atmospheric Chemistry and Physics*, 13, 2,757–2,777. https://doi.org/10.5194/acp-13-2757-2013
- Cummins, K. L., & Murphy, M. J. (2009). An overview of lightning locating systems: History, techniques, and uses, with an in-depth look at the U.S. NLDN. *IEEE Transactions on Electromagnetic Compatibility*, *51*, 499–518.
- Cummins, K. L., Murphy, M. J., Bardo, E. A., Hiscox, W. L., Pyle, R. B., & Pifer, A. E. (1998). A combined TOA/MDF technology upgrade of the U.S. national lightning detection network. *Journal of Geophysical Research*, 103, 9,035–9,044. https://doi.org/10.1029/98JD00153
- Cummins, K. L., Cramer, J. A., Biaji, C. J., Krider, E. P., Jerauld, J., Uman, M. A., & Rakov, V. A. (2006). The U.S. national lightning detection network: Post-upgrade status. preprints, 2nd Conference on Meterological Applications of Lightning Data (9 pp.). Atlanta, GA: American Meteorological Society. 29 Jan. 2 Feb.
- DeCaria, A. J., Pickering, K. E., Stenchikov, G. L., Scala, J. R., Stith, J. L., Dye, J. E., ... Laroche, P. (2000). A cloud-scale model study of lightning-generated NO_X in an individual thunderstorm during STERAO-A. *Journal of Geophysical Research*, 105, 11,601–11,616. https://doi.org/10.1029/2000JD900033
- DeCaria, A. J., Pickering, K. E., Stenchikov, G. L., & Ott, L. E. (2005). Lightning-generated NO_X and its impact on tropospheric ozone production: A three-dimensional modeling study of a stratosphere-troposphere experiment: Radiation, aerosols and ozone (STERAO-A) thunderstorm. Journal of Geophysical Research, 110, D14303. https://doi.org/10.1029/2004JD005556
- DiGangi, E. A., MacGorman, D. R., Ziegler, C. L., Betten, D., Biggerstaff, M., Bowlan, M., & Potvin, C. (2016). An overview of the 29 May 2012 Kingfisher supercell during DC3. *Journal of Geophysical Research: Atmospheres, 121*, 14,316–14,343. https://doi.org/10.1002/2016JD025690
- Goodman, S. J., Blakeslee, R., Christian, H., Koshak, W., Bailey, J., Hall, J., ... Gatlin, P. (2005). The north Alabama lightning mapping array: Recent severe storm observations and future prospects. *Atmospheric Research*, *76*, 423–437. https://doi.org/10.1016/j.atmosres.2004.11.035
- Grenier, P., Parent, A.-C., Huard, D., Anctil, F., & Chaumont, D. (2013). An assessment of six dissimilarity metrics for climate analogs. *Journal of Applied Meteorology and Climatology*, 52, 733–752. https://doi.org/10.1175/JAMC-D-12-0170.1
- Koshak, W. J., Solakiewicz, R. J., Blakeslee, R. J., Goodman, S. J., Christian, H. J., Hall, J. M., ... Cecill, D. J. (2004). North Alabama lightning mapping array (LMA): VHF source retrieval algorithm and error analyses, *Journal of Atmospheric and Oceanic Technology*, 21, 543–558. https://doi.org/10.1175/1520–0426(2004)021<0543:NALMAL>2.0.CO;2
- Koshak, W. J., Biazar, A. P., Khan, M. N., & Wang, L. (2014). The NASA lightning nitrogen oxides model (LNOM): Application to air quality modeling. *Atmospheric Research*, 135–136, 363–369. https://doi.org/10.1016/j.atmosres.2012.12.015
- Lang, T. J., Cummer, S. A., Rutledge, S. A., & Lyons, W. A. (2013). The meteorology of negative cloud-to-ground lightning strokes with large charge moment changes: Implications for negative sprites. *Journal of Geophysical Research: Atmospheres, 118,* 7,886–7,896. https://doi.org/10.1002/jgrd.50595
- Lu, G., Cummer, S. A., Blakeslee, R. J., Weiss, S., & Beasley, W. H. (2012). Lightning morphology and impulse charge moment change of high peak current negative strokes. *Journal of Geophysical Research*, 117, D04212. https://doi.org/10.1029/2011JD016890
- Maggio, C., Coleman, L., Marshall, T., & Stolzenburg, M. (2005). Lightning-initiation locations as a remote sensing tool of large thunderstorm electric field vectors. *Journal of Oceanic and Atmospheric Technology*, 22, 1059–1068. https://doi.org/10.1175/JTECH1750.1
- Maia, A. H. N., Meinke, H., Lennox, S., & Stone, R. C. (2007). Inferential, non-parametric statistics to assess quality of probabilistic forecast systems. *Monthly Weather Review*, 135, 351–362. https://doi.org/10.1175/MWR3291.1
- Mallick, S., Rakov, V. A., Hill, J. D., Ngin, T., Gamerota, W. R., Pilkey, J. T., ... Nag, A. (2014). Performance characteristics of the NLDN for return strokes and pulses superimposed on steady currents, based on rocket-triggered lightning data acquired in Florida in 2004–2012. *Journal of Geophysical Research: Atmospheres, 119*, 3,825–3,856. https://doi.org/10.1002/2013JD021401
- Mecikalski, R. M., & Carey, L. D. (2017). Lightning characteristics relative to radar, altitude and temperature for a multicell, MCS and supercell over northern Alabama. Atmospheric Research, 191, 128–140. https://doi.org/10.1016/j.atmosres.2017.03.001
- Mecikalski, R. M., Bain, A. L., & Carey, L. D. (2015). Radar and lightning observations of deep moist convection across northern Alabama during DC3: 21 May 2012. Monthly Weather Review, 143, 2,774–2,794. https://doi.org/10.1175/MWR-D-14-00250.1
- Ott, L. E., Pickering, K. E., Stenchikov, G., Huntrieser, H., & Schumann, U. (2007). Effects of lightning NO_X production during the 21 July European lightning nitrogen oxides project storm studied with a three-dimensional cloud-scale chemical transport model. *Journal of Geophysical Research*, 112, D05307. https://doi.org/10.1029/2006JD007365
- Ott, L. E., Pickering, K. E., Georgiy, L., Stenchikov, G. L., Allen, D. J., DeCaria, A. J., ... Tao, W.-K. (2010). Production of lightning NO_x and its vertical distribution calculated from three-dimensional cloud-scale chemical transport model simulations. *Journal of Geophysical Research*, 115, D04301. https://doi.org/10.1029/2009JD011880
- Pickering, K. E., Wang, Y., Tao, W. K., Price, C., & Müller, J.-F. (1998). Vertical distributions of lightning NO_x for use in regional and global chemical transport models. *Journal of Geophysical Research*, 103, 31.203–31.216. https://doi.org/10.1029/98JD02651
- Pollack, I. B., et al. (2016). Airborne quantification of upper tropospheric NOx production from lightning in deep convective storms over the United States Great Plains. *Journal of Geophysical Research: Atmospheres, 121,* 2002–2028. https://doi.org/10.1002/2015JD023941
- Press, W. H., Teukolsky, S. A., Vetterling, W. T., & Flannery, B. P. (1992). Numerical Recipes in C: The Art of Scientific Computing, 2nd ed. (994 pp.). Cambridge: Cambridge Univ. Press.
- Qie, X., Wang, Z., Wang, D., & Liu, M. (2013). Characteristics of positive cloud-to-ground lightning in Da Hinggan Ling forest region at relatively high latitude, northeastern China. *Journal of Geophysical Research: Atmospheres, 118*, 13,393–13,404. https://doi.org/10.1002/2013JD020093
- Ridley, B. A., Dye, J. E., Walega, J. G., Zheng, J., Grahek, F. E., & Rison, W. (1996). On the production of active nitrogen by thunderstorms over New Mexico. *Journal of Geophysical Research*, 101, 20,985–21,005. https://doi.org/10.1029/96JD01706
- Schumann, U., & Huntrieser, H. (2007). The global lightning-induced nitrogen oxides source. *Atmospheric Chemistry and Physics*, 7, 3,828–3,907. https://doi.org/10.5194/acp-7-3823-2007
- Skamarock, W. C., Dye, J. E., Defer, E., Barth, M. C., Stith, J. L., Ridley, B. A., & Baumann, K. (2003). Observational and modeling-based budget of lightning-produced NO_x in a continental thunderstorm. *Journal of Geophysical Research*, 108(D10), 4,305. https://doi.org/10.1029/2002JD002163



Geophysical Research Letters

- Stith, J. L., Basarab, B., Rutledge, S. A., & Weinheimer, A. (2016). Anvil microphysical signatures associated with lightning-produced NO_x. Atmospheric Chemistry and Physics, 16, 2,243–2,254. https://doi.org/10.5194/acp-16-2243-2016
- Thomas, R., Krehbiel, P., Rison, W., Harlin, J., Hamlin, T., & Campbell, N. (2003). The LMA flash algorithm, *Proc. 12th Int. Conf. On Atmospheric Electricity* (pp. 655–656). Versailles, France: International Commission on Atmospheric Electricity.
- Wilks, D. S. (2006). Statistical Methods in the Atmospheric Sciences, 2nd ed. (627 pp.). Academic Press: Amsterdam.
- Zhang, Y., Zhang, Y., Zheng, D., & Lu, W. (2015). Preliminary breakdown, following lightning discharge processes and lower positive charge region. *Atmospheric Research*, 161–162, 52–56. https://doi.org/10.1016/j.atmosres.2015.03.017